ISSN 1063-7826, Semiconductors, 2009, Vol. 43, No. 3, pp. 323–330. © Pleiades Publishing, Ltd., 2009.
Original Russian Text © S.P. Kozyrev, 2009, published in Fizika i Tekhnika Poluprovodnikov, 2009, Vol. 43, No. 3, pp. 342–348.

LOW-DIMENSIONAL SYSTEMS

# Infrared Spectroscopy of Lattice Vibrations in ZnTe/CdTe Superlattices with Quantum Dots on the GaAs substrate with the ZnTe buffer layer

**S. P. Kozyrev^**

*Lebedev Physical Institute, Russian Academy of Sciences, Moscow, 119991 Russia*
*^e-mail: skozyrev@sci.lebedev.ru*

Submitted May 12, 2006; accepted for publication May 19, 2008

**Abstract**—The results of the analysis of the infrared lattice reflectance spectra of multiperiod ZnTe/CdTe superlattices with CdTe quantum dots are reported. The samples are grown by molecular beam epitaxy on the GaAs substrate with the ZnTe buffer layer. Due to the large number of periods of the superlattices, it is possible to observe CdTe-like vibration modes in the quantum dots, i.e., the dislocation-free stressed islands formed during the growth due to relaxation of elastic stresses between the ZnTe and CdTe layers are markedly different in their lattice parameters. From the frequency shifts of the CdTe- and ZnTe-like vibration modes with respect to the corresponding modes in the unstressed materials, it is possible to estimate the level of elastic stresses.

PACS numbers: 78.67.Hc, 78.40.Fy

**DOI:** 10.1134/S1063782609030129

## 1. INTRODUCTION

In the growth of multilayered structures (e.g., superlattices) in the system of materials with a pronounced mismatch between the lattice parameters (lattice constants), elastic stresses play a decisive role in the formation of the region between the adjacent layers, i.e., the interface region. For each pair of materials of adjacent layers, the concept of the critical thickness is introduced. When a superlattice is grown of layers with the thickness larger than the critical thickness, the elastic stresses produced at the initial stage of growth because of the lattice mismatch between the adjacent layers relax via the formation of misfit dislocations, and the constituent layers of such superlattice possesses the properties of the unstressed bulk material. If the layer's thickness is smaller than the critical thickness, the elastic strains persist in the superlattice, and the superlattice itself can be grown coherent to the substrate or buffer layer; i.e., the lattice parameters in the plane of growth can be the same for the whole superlattice structure. For such superlattices, the very high quality of interfaces is typical. When a superlattice is grown with thin layers of one material (with the thickness close to the critical thickness or smaller) on thick layers of the other material, another mechanism of relaxation of elastic strains is possible: the stresses relax via the formation of dislocation-free strained islands in the thin layers (see, e.g., [1, 2] and references therein). In this case, if the thin layers are formed of an alloy, the islands are markedly different in composition from the layer, and the elastic-strain-induced segregation of particular components in the islands favors a sharp increase in the rate of growth. These effects present many problems in growing traditional planar electronic devices, but the same effects are now used to fabricate structures with self-assembled quantum dots (QDs). It is the elastic strains produced during the growth of such structures that are responsible for the formation of island QDs and their shape and electronic structure. In this regard, of interest are the properties of multilayered QD structures based on the CdTe/ZnTe pair of semiconductor materials. The specific feature of the CdTe/ZnTe heteropair is that the potential offset in the valence band is almost totally controlled by the elastic strains produced because of the well-pronounced lattice mismatch between CdTe and ZnTe [3]. Variations in the distribution of elastic strains under variations in the structural characteristics, such as the material of the buffer layer or the thickness of the ZnTe barrier layers sandwiching the CdTe QD layer, provide an additional opportunity for controlling the electronic properties of the structure up to changing the type of the energy-band diagram. For example, the authors of [4] faced an unusual situation: a superlattice with CdTe QD layers and thin ZnTe barrier layers on a thick buffered CdTe layer exhibited a photoluminescence spectrum that involved the two types of exciton states, specifically, the spatially direct and spatially indirect states.

Previously, using long-wavelength infrared (IR) spectroscopy [5] and photoluminescence measurements [6], we studied the vibration states and electron states in the structures of multiple CdTe QD planes sandwiched between ZnTe barrier layers. These structures are referred to as the QD superlattices (QDSLs).

**Table 1.** Parameters of the QDSL structures

| Structure | b05 | b50 | b0 | b10.20 | b10.200 |
|---|---|---|---|---|---|
| Buffer layer | ZnTe | ZnTe | ZnTe(+CdTe) | ZnTe(+CdTe) | ZnTe(+CdTe) |
| CdTe layer thickness, ML | 3 | 3 | 3 | 3 | 3 |
| ZnTe spacer thickness, ML | 5 | 50 | – | 10 | 10 |
| Number of CdTe layer | 400 | 100 | 1 | 20 | 200 |

The QDSLs were gown by molecular beam epitaxy on the GaAs (100) substrates with the thick CdTe layer. The QDSLs involved 200 periods of the CdTe layers, with the nominal growth thickness of 2.5 monolayers (ML), and the separating ZnTe barriers with the thickness ranging from 12 to 75 ML. The structures grown in such a manner were analyzed by transmittance electron microscopy (TEM) in the direction of growth. The TEM data showed [7] that the individual CdTe QD layer was the $Zn_{1-x}Cd_xTe$ alloy layer, in which islands with an increased CdTe content were distributed; the islands were 10 nm in diameter and about 2 nm wide. If the thickness of the ZnTe barrier layer was smaller than 25 ML, we observed a correlation between different CdTe QD layers in the arrangement of the islands. The correlated arrangement of the islands was observed in the individual layers as well. Depending on the thickness of the ZnTe barrier layer (and the corresponding distribution of elastic strains in the structure), the photoluminescence spectrum [6] was controlled either by spatially indirect excitonic transitions for the structures with thick barrier layers or by the two types of excitonic transitions (spatially indirect and spatially direct transitions) for the structures with small thicknesses of the ZnTe barrier layers.

IR spectroscopy of lattice vibrations [5] made it possible to assess the distribution of elastic strains in the QDSL structures from the shifts of vibrational eigenfrequencies for materials forming these structures. The QDSL structures on the substrates with the CdTe buffer layer [5] exhibited intense reflectance bands related to vibrational excitations in the GaAs substrate, ZnTe barrier layers and CdTe buffer layer. It was found that an additional mode split off from the basic mode of ZnTe, and this splitting was attributed to the manifestation of the ZnTe-like mode of the ZnCdTe alloys formed in the CdTe QD layer due to interdiffusion of Zn and Cd at the interfaces. Observation of the mode of vibrational excitation of the CdTe QDs was impossible because it was efficiently screened by the mode of the thick CdTe buffer layer. Analysis of the IR lattice reflectance from the structures with the multiple CdTe QD planes between ZnTe barrier layers showed that, in the structures with thicker barrier layers (25 ML and thicker) between the CdTe QD planes, the elastic strains are concentrated in the $Zn_{1-x}Cd_xTe$ alloy layers. In the case of a thin ZnTe layer (12 ML and thinner), the distribution pattern of elastic strains is more complex, since the influence of the thick CdTe buffer layer extends over the entire QDSL structure, if the structure consists of the CdTe QD layers separated by thin ZnTe barriers.

In this study, we continued investigating the structures of multiple CdTe QD planes between the ZnTe layers with different thickness. The structures are grown on the GaAs substrate with the thick ZnTe buffer layer. The replacement of the CdTe buffer layer by the ZnTe buffer layer allows us to observe the modes of vibrational excitation of CdTe QDs (in reality, the modes of the CdZnTe alloy enriched with CdTe) that exhibit the eigenfrequencies substantially shifted with respect to those in the bulk. In this case, the frequency shift is controlled by large elastic strains rather than by the change in the dimensionality of the layer. The use of the ZnTe buffer layer instead of CdTe layer yields a significant change in the spectra of vibrational excitations and, correspondingly, in the distribution of elastic strains in the similar CdTe/ZnTe QDSL, when formed on the other buffer layer. The results of the analysis of the reflectance spectra of the IR lattice for the QDSL structures formed on the substrate with the ZnTe buffer layer (specifically, the observation of the ~150 $cm^{-1}$ mode corresponding to the CdTe-like vibration in the CdTe QD layer) were partially reported in [8] were concerned with the vibrational and electronic states in the QDSL structures grown on the GaAs substrate with the ZnTe buffer layer. In what follows, we use the data on the photoluminescence spectra of the QDSL structures from [8].

## 2. DISPERSION ANALYSIS OF THE REFLECTANCE SPECTRA OF THE IR LATTICE

The QD structures were grown by molecular beam epitaxy on the semi-insulator GaAs (100) substrates with the 5-μm-thick ZnTe buffer layer. The substrate temperature was 350°C. The QDSL structure consisted of different numbers of CdTe layers separated by ZnTe barrier layers. In different samples, the thickness of nominal growth was 3 ML for the CdTe layers and 5–40 ML for the ZnTe barrier layers. The protective ZnTe layer with the thickness 40 nm was deposited onto the top of the structure. The technology of growth of the QDSL structures was described previously [5, 7]. The parameters and labels of the structures to be studied were the same as in [8] (Table 1).

The long-wave IR reflectance spectra were recorded at 300 K with the use of a Bruker IFS 113v Fourier

spectrometer with the spectral resolution about 1 $cm^{-1}$. The further discussion is concerned with the analysis of lattice vibrations, whose spectrum is experimentally obtained basically from the long-wavelength IR reflectance. Therefore, we must now mention some features of the lattice vibration spectroscopy as a technique that provides interaction of crystal lattice vibrations with IR radiation at the wavelength 30–80 μm. To provide optimal conditions of the studies of lattice vibrations, the thickness of the structure grown on a thick substrate must be chosen at 2–5 μm. It is for this reason that, because of the inadequate sensitivity of the technique, it is unfortunately impossible to study short-period QDSLs: it is necessary to grow periodic structures with the number of periods close to 100. The IR lattice reflectance spectrumpresents an integrated characterization of all constituent layers of the structure and the substrate.

Figure 1 shows the lattice's reflectance spectra of two QDSL samples, **b05** and **b50**, on the GaAs substrate with the ZnTe buffer layer with the thickness ~5 μm. Figure 1 also shows the lattice's reflectance spectrum for the elastically strained ZnTe(10 nm)/$Zn_{0.8}Cd_{0.2}Te$ (6 nm) superlattice of 100 layers (sample **SL**) on the GaAs substrate with the 1.3-μm-thick ZnTe buffer layer, as reported in [9]. For clarity, the spectra are slightly shifted from each other along the ordinate axis. Except for the ~150 $cm^{-1}$ region of CdTe-like vibrations lacking in the spectrum of ZnTe/$Zn_{0.8}Cd_{0.2}Te$ sample **SL**, all features of the spectra of the QDSL samples **b05**, **b50**, and sample **SL** are identical. The 269 $cm^{-1}$ mode corresponds to the lattice's vibration mode of bulk GaAs, and the ~177 $cm^{-1}$ mode is a superposition of two ZnTe-like vibration modes. In [9], it was shown that the ZnTe/$Zn_{0.8}Cd_{0.2}Te$ sample **SL** was elastically strained, with sharp interfaces between the layers. In the ZnTe layers when experiencing an extending stress, the vibration eigenfrequency is changed from 179 to 176 $cm^{-1}$, and in the $Zn_{0.8}Cd_{0.2}Te$ layers influenced by compressing stresses, the frequency increases from 173 to 177 $cm^{-1}$. The lattice's vibration frequencies in the elastically strained layers of superlattice **SL** are close to each other, and with the damping parameter of lattice modes $\gamma \approx 3$ $cm^{-1}$, these modes are not resolved even at the liquid-helium temperature [9]. From the similarity of the lattice's vibration spectra of QD samples **b05** and **b50** and sample **SL**, it follows that, when the CdTe layer in the QDSL structures under consideration is grown on the thicker ZnTe layer, the ZnCdTe alloy layer graded in composition (rather than the CdTe layer) is formed. According to [2], relaxation of elastic strains in this alloy layer is accompanied by the formation of ZnCdTe islands with the enhanced segregation of CdTe. These islands are distributed in the layer, whose prevailing composition is close to $Zn_{0.8}Cd_{0.2}Te$. The ~150 $cm^{-1}$ mode in the QDSL corresponds to the CdTe-like vibration of the QDs, i.e., the ZnCdTe islands enriched with CdTe.

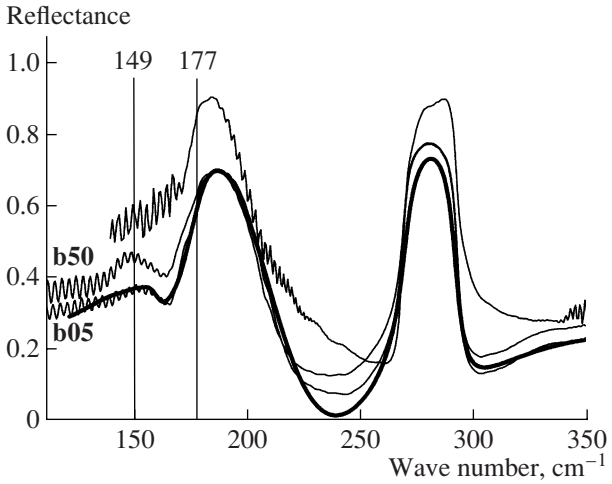


**Fig. 1.** Lattice reflectance spectra for QDSL structures **b05** and **b50** on the GaAs substrate with the ZnTe buffer layer and for the strained ZnTe/$Zn_{0.8}Cd_{0.2}Te$ superlattice (sample **SL**) on the GaAs substrate with the ZnTe buffer layer [9]. For clarity, the spectra are shifted from each other along the ordinate axis. Thick line refers to the spectrum calculated for structure **b05**.

To carry out the dispersion analysis of the lattice's reflectance spectra of the superlattices, we used the model structure formed by a thin film (the superlattice + buffer layer) on the top of a bulk (semi-infinite) substrate. In the context of such a model's structure, for the film with the thickness $L$ and the permittivity function $\varepsilon_f(\omega)$ and for the substrate with the permittivity $\varepsilon_s(\omega)$, the amplitude's reflectivity in the case of normal incidence of light is [10]

$$r_{1fs}(\omega) = \frac{r_{1f}(\omega) + r_{fs}(\omega)\exp(i2\beta)}{1 + r_{1f}(\omega)r_{fs}(\omega)\exp(i2\beta)}, \qquad (1)$$

where

$$r_{1f}(\omega) = \frac{1 - \sqrt{\varepsilon_f(\omega)}}{1 + \sqrt{\varepsilon_f(\omega)}},$$

$$r_{fs}(\omega) = \frac{\sqrt{\varepsilon_f(\omega)} - \sqrt{\varepsilon_s(\omega)}}{\sqrt{\varepsilon_f(\omega)} + \sqrt{\varepsilon_s(\omega)}} \text{ and } \beta = \frac{2\pi L\sqrt{\varepsilon_f(\omega)}}{\lambda}.$$

Here, $\lambda$ is the wavelength (= 10000/$\omega$). The reflectance is $R(\omega) = |r_{1fs}(\omega)|^2$. In the model calculation, we disregard multiple scattering at the interfaces, since the corresponding expression is rather cumbersome and do not provide any additional data on lattice vibrations in the film, except for the data on the interference effects. In Fig. 1, the interference in the GaAs substrate with the thickness ~500 μm manifests itself as frequent oscillations with a period of about 2.5 $cm^{-1}$ in the transparency region of the substrate and film (the superlattice + buffer layer).

**Table 2.** Lattice vibration parameters (frequencies $\omega_{tj}$, oscillator strengths $S_j$, and damping parameters $\gamma_j$) obtained by dispersion analysis of the lattice's reflectance spectra

| Structure | **b05** | **b50** | **b0** | **b10.20** | **b10.200** |
|---|---|---|---|---|---|
| Substrate GaAs | 269/1.8/6 | 269/1.9/5 | 267/1.9/11 | 267/1.9/12 | 267/1.9/12 |
| $\omega_t$, cm$^{-1}$/$S$/$\gamma$, cm$^{-1}$ | | | | | |
| CdTe-like modes | 150/0.8/12 | 149/0.4/13 | 149/0.5/9 | 149/0.55/11 | 149/0.5/14 |
| $\omega_t$, cm$^{-1}$/$S$/$\gamma$, cm$^{-1}$ | 157/0.25/11 | 156/0.5/13 | | 144/0.2/7 | 144/0.2/7 |
| ZnTe-like modes | 174/1.2/13 | 175/1.1/8 | 168/0.07/7 | 168/0.15/8 | 170/0.3/9 |
| $\omega_t$, cm$^{-1}$/$S$/$\gamma$, cm$^{-1}$ | 178/0.7/10 | 179/0.8/11 | 179/0.5/7.5 | 178.5/0.6/10 | 177/0.7/11 |

Note: The frequencies of TO vibration modes in bulk GaAs, CdTe, and ZnTe are $\omega_t$ = 270, 140, and 179 cm$^{-1}$, respectively.

The permittivity function of the film, $\varepsilon_f(\omega)$, is expressed in the classical additive form:

$$\varepsilon_f(\omega) = \varepsilon_\infty + \sum_j \frac{S_j \omega_{tj}^2}{\omega_{tj}^2 - \omega^2 - i\omega\gamma_j}. \quad (2)$$

In calculating the reflectance $R(\omega)$, we varied the frequency of the $j$th TO mode $\omega_{tj}$ in formula (2) for $\varepsilon_f(\omega)$, the oscillator strength of this mode $S_j$, and its damping parameter $\gamma_j$. The results of the dispersion analysis for QDSL samples **b05** and **b50** are summarized in Table 2.

Two CdTe-like vibration modes in the QDs are evident at the frequencies ~150 and ~156 cm$^{-1}$ corresponding to the groups of small and large CdTe-enriched ZnCdTe islands observable for QDSLs in the TEM measurements [7]. The content of components in the composition of the QDs (the degree of segregation of CdTe) and, correspondingly, the elastic strains in the QDs are different, depending on the QD dimensions. The magnitude of the elastic strains controls the frequency shift of lattice vibrations.

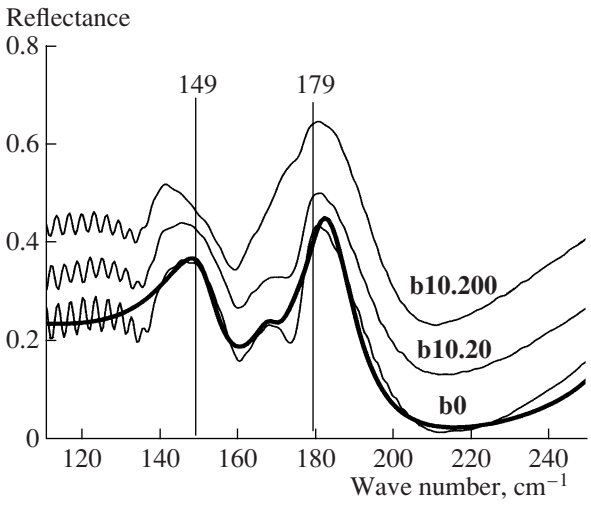


**Fig. 2.** Lattice reflectance spectra for QDSL structures **b10.20** and **b10.200** on the GaAs substrate with the ZnTe (+ CdTe) buffer layer and for the GaAs substrate with the ZnTe (+ CdTe) buffer layer (sample **b0**). For clarity, the spectra are shifted from each other along the ordinate axis. Thick line refers to the spectrum calculated for structure **b05**.

Figure 2 shows the lattice's reflectance spectra of QDSL structures **b10.20** and **b10.200** on the GaAs substrate with the ZnTe buffer layer with the thickness ~5 μm. The parameters of these structures are the same as in [8], as listed in Table 1. In structures **b10.20** and **b10.200**, thin CdTe layers are arranged between the ZnSe barrier layers with the same growth thickness 10 ML; structures **b10.20** and **b10.200** differ only in the number of periods (20 and 200, respectively). Figure 2 also shows the lattice's reflectance spectrum of sample **b0**, i.e., the GaAs substrate with the ZnTe buffer layer, on which one thin CdTe layer and the protective 40-nm-thik ZnTe layer were deposited. From the standpoint of lattice reflectance, sample **b0** is merely the GaAs substrate with the ZnTe buffer layer, and it is insensitive to the rest of the IR spectrum. However, in analyzing the lattice's reflectance spectra of sample **b0**, we found that there existed an extra CdTe layer with the thickness ~1 μm between the GaAs substrate and ZnTe buffer layer with the thickness ~5 μm. Later, this result was supported by additional studies. The 149 cm$^{-1}$ lattice vibration mode (Fig. 2) different from the 140 cm$^{-1}$ mode for unstrained CdTe corresponds to this CdTe extra layer. This 149 cm$^{-1}$ mode is evident also in the spectra of QDSL samples **b10.20** and **b10.200**. The extra CdTe layer (the lattice parameter $a$ = 6.48 Å) is in the highly compressed state between the GaAs substrate ($a$ = 5.56 Å) and thick ZnTe buffer layer ($a$ = 6.10 Å) because of the large difference between the lattice parameters. The highly compressed buried CdTe layer induces a frequency shift of the lattice mode of the thick GaAs substrate from $\omega_t$ = 269 to 267 cm$^{-1}$ and promotes the appearance of an extra strained region (the peak at $\omega_t$ = 168 cm$^{-1}$) in the ZnTe buffer layer. The basic mode of the ZnTe buffer layer is at $\omega_t$ = 179 cm$^{-1}$. When compared to the lattice's reflectance spectrum of sample **b0**, the spectra of QDSL structures **b10.20** and **b10.200** exhibit additional modes at $\omega_t$ = 144 cm$^{-1}$

**Table 3.** Parameters used in calculations of relative shift of the frequency of vibrational TO mode $\Delta\omega_t/\omega_t$ (the shift is induced by elastic stresses)

| $Cd_{1-x}Zn_xTe$ | $a$, Å | $C_{11}$, $10^{11}$ dyn/cm$^2$ | $C_{12}$, $10^{11}$ dyn/cm$^2$ | $e^*$ | $\omega_t$, cm$^{-1}$ | $\omega_l$, cm$^{-1}$ |
|---|---|---|---|---|---|---|
| $x = 0$ (CdTe) | 6.482 | 5.35 | 3.68 | 0.867 | 141 | 171 |
| $x = 0.3$ CdTe-like | 6.369 | 5.88 | 3.80 | 0.837 | 143 | 161 |
| $x = 0.5$ CdTe-like | 6.293 | 6.235 | 3.87 | 0.816 | 144.5 | 157.5 |
| $x = 0.5$ ZnTe-like | 6.293 | 6.235 | 3.87 | 0.816 | 172 | 185 |
| $x = 0.8$ ZnTe-like | 6.180 | 6.765 | 3.99 | 0.785 | 174 | 196 |
| $x = 1$ (ZnTe) | 6.104 | 7.12 | 4.07 | 0.766 | 179 | 206 |

(the modes of the CdTe QDs) and $\omega_t = 169$ cm$^{-1}$ (the ZnTe-like vibration modes of the ZnCdTe layer). The data of the dispersion analysis of the IR lattice reflectance for QDSL structures **b10.20** and **b10.200** on the GaAs substrate with the combined ZnTe (+CdTe) buffer layer and for sample **b0**, i.e., the GaAs substrate itself with the ZnTe(+CdTe) buffer layer are summarized in Table 2.

In the previous study [8] concerned with electron states and vibration states in the same QDSL structures on the GaAs substrate with the ZnTe buffer layer, as those studied here, the authors reported a sharp difference between two seemingly similar structures **b05** and **b10.200** in intensity, shape and position of the bands in the photoluminescence spectrum. One structure, **b05**, consists of 400 ML of CdTe between the ZnTe layers with the thickness 0.5 ML, and the other, **b10.200**, consists of 200 ML of CdTe between the ZnTe layers with the thickness 10 ML. The comprehensive analysis of the lattice's reflectance spectra of structures **b05** and **b10.200** suggests that structure **b05** was formed on the ZnTe buffer layer, whereas structure **b10.200** was formed on the ZnTe(+CdTe) buffer layer with the buried CdTe layer. The frequencies of the CdTe-like vibrations in the QDs are $\omega_t \approx 150$ and 156 cm$^{-1}$ for structure **b05** and $\omega_t \approx 144$ cm$^{-1}$ for structure **b10.200** (for unstrained CdTe, the frequency is $\omega_t \approx 140$ cm$^{-1}$). The above difference is representative of the difference between the distributions of elastic strains in the structures on the substrates with the ZnTe and ZnTe (+CdTe) buffer layers. It is noteworthy that the frequencies $\omega_t$ of the lattice vibration modes in the CdTe QD layers of the QDSL structures with the same buffer layers depend only slightly on the ZnTe barrier's thickness.

## 3. CALCULATION OF THE STRAIN-INDUCED SHIFT OF OPTICALLY ACTIVE LATTICE VIBRATION MODES IN QDSLs

In discussing the results of the dispersion analysis of the lattice's reflectance spectra of the QDSL structures in Section 2, we assume that the shifts of vibration modes of the layers in the structures were induced by elastic strains between the layers of the superlattices. Now we estimate the elastic-strain-induced frequency shift $\Delta\omega_t$ of the transverse vibration modes in the layers, $\omega_t$, theoretically. We start from the relations [11]

$$\frac{\Delta\omega_t}{\omega_t} = \frac{1}{2(1-\gamma^*)}\left[\frac{\Delta K_t}{K_0} - \gamma^*(\delta_v + \delta_d)\right] \approx \frac{1}{2(1-\gamma^*)}\frac{\Delta K_t}{K_0} = k\left(-\frac{\Delta a}{a}\right), \quad (3)$$

where

$$\frac{\Delta K_t}{K_0} = \left(1 - \frac{2\rho}{R_0}\right)^{-1} \times \left[\frac{2R_0}{3\rho}\left(1 - \frac{C_{12}}{C_{11}}\right) - \frac{2}{3}\left(1 + \frac{2C_{12}}{11}\right) - \frac{2\rho}{R_0}\right]\left(-\frac{\Delta a}{a}\right),$$

$$\frac{R_0}{\rho} = 16\sqrt{3}B\frac{R_0^4}{\alpha(e)^2} + 2, \quad B = (C_{11} + 2C_{12})/3,$$

$$\alpha = 1.6381, \text{ and } \gamma^* = [(\omega_l/\omega_t)^2 - 1]/[(\omega_l/\omega_t)^2 + 2].$$

Here, $a$ and $\Delta a$ are the lattice constant and its change in the plane of the layers, respectively. In [11], the calculation was performed in the context of the model of rigid ions. The ratio $\rho/R_0$ is the ratio of the repulsive potential parameter to the distance $R_0$ ($= a\sqrt{3}/4$) between the nearest neighbors in the unstrained material, $C_{11}$ and $C_{12}$ are the elastic constants, $B$ is the bulk elasticity modulus, $e^*$ is the effective ion's charge, and $\omega_t$ and $\omega_l$ are the transverse and longitudinal phonon frequencies. The term $\gamma^*(\delta_v + \delta_d)$ in Eq. (3) takes into account the changes in the contributions of Coulomb interaction to the frequency shift under the changes in the volume of the unit cell and in the depolarization factors. This term is small compared to $\Delta K_t/K_0$ defined by the parameter $\rho/R_0$. Disregard of this term gives an error not exceeding 10%.

The lattice constants $a$, the elastic constants $C_{11}$ and $C_{12}$ and the effective ion's charge $e^*$ are listed in Table 3. The parameters of CdTe ($x = 0$) and ZnTe ($x = 1$) were

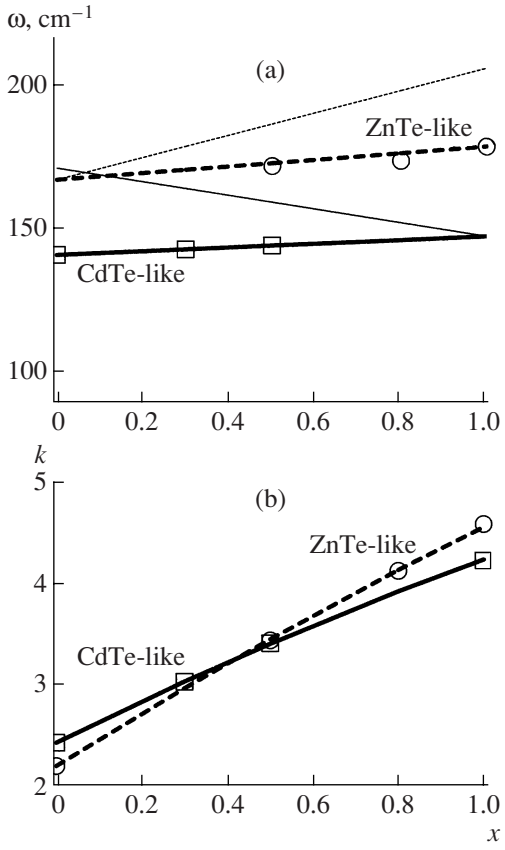


**Fig. 3.** (a) Frequencies of (solid lines) the CdTe- and (dashed lines) ZnTe-like TO and LO vibration modes in the $Cd_{1-x}Zn_xTe$ alloy versus the composition parameter $x$ at $T = 300$ K [13]. Thick and thin lines refer to the TO and LO modes, respectively. (b) The calculated coefficient of proportionality $k$ between the strain $\Delta a/a$ and the relative frequency shift of (solid line) the CdTe- and (dashed line) ZnTe-like vibration mode $\Delta\omega_t/\omega_t$ versus the composition parameter $x$. Symbols (open circles and squares) refer to the values of $k$ for the compositions $x$, for which the coefficient $k$ was calculated.

used in [12] in the calculations concerned with the crystal lattice dynamics and phonon dispersion and performed in the context of the 11-parameter model of hard ions to interpret the data of neutron scattering. For the $Cd_{1-x}Zn_xTe$ alloy with the composition parameter $x$, the calculated parameters were interpolated by the formula $C(x) = (1 - x)C^{CdTe} + xC^{ZnTe}$, where $C$ means the elastic constants $C_{11}$ and $C_{12}$. Figure 3a shows the dependence of the frequencies of TO and LO modes of the CdTe- and ZnTe-like vibrations in the $Cd_{1-x}Zn_xTe$ alloy on the composition parameter $x$ at $T = 300$ K [13]. Figure 3b shows the dependence of the coefficient of proportionality $k$ between the strain $\Delta a/a$ and the relative frequency shift of the vibration mode $\Delta\omega_t/\omega_t$ for CdTe- and ZnTe-like vibrations in the $Cd_{1-x}Zn_xTe$ alloy on the composition parameter $x$.

The lattice constant of the layers in the lateral direction, $a^{\perp}$, was estimated in the approximation of equilibrium of two elastic layers 1 and 2 pulled one (1) over the other (2), with free surfaces [14]:

$$a^{\perp} = \frac{n_1 a_1^2 K_1 + n_2 a_2^2 K_2}{n_1 a_1 K_1 + n_2 a_2 K_2},$$
$$K_i = \frac{1}{S_{11i} + S_{12i}}, \quad i = 1, 2. \tag{4}$$

Here, $n_i$ is the number of elastic layers, $a_i$ is the lattice constant of the $i$th layer, $S_{11}$ and $S_{12}$ are the elastic moduli related to the elastic constants by the relations

$$S_{11} - S_{12} = \frac{1}{C_{11} - C_{12}}$$

and

$$S_{11} + 2S_{12} = \frac{1}{C_{11} + 2C_{12}}.$$

In what follows, the results of measurements are interpreted with regard to the conclusions from TEM structural analysis of the CdSe/ZnSe nanostructures [15]. The CdSe/ZnSe and CdTe/ZnTe nanostructures are similar in many respects (structure, lattice vibration properties, etc.), but the CdSe/ZnSe nanostructures are now better understood. In studying the CdSe layers with the growth thickness from 0.5 to 3.0 ML in the structure, in which the layers were buried in the ZnSe matrix, the authors of [15] detected the two-dimensional (2D) $Zn_{1-x}Cd_xSe$ layers with the thickness ~3 nm, i.e., ~10 ML for all of the samples, irrespective to the growth thickness of the CdSe layer (the thickness was estimated as the width of the concentration profile at its half-maximum). These $Zn_{1-x}Cd_xSe$ layers contained inclusions (islands) with a high Cd content; in lateral dimensions, these islands were distributed to form two groups, small-sized (≤10 nm) islands and large-sized (30–130 nm) islands. The height of the islands did not exceed the thickness of the $Zn_{1-x}Cd_xSe$ layer. The composition of the 2D $Zn_{1-x}Cd_xSe$ layer and the islands enriched with CdSe was defined by the thickness of initially grown CdSe.

For all of the QDSL structures studied here, the growth thickness of the CdTe layer in the superlattice is the same, 3 ML. From the TEM analysis of the samples similar to those considered here [7], the thickness of the $Zn_{1-x}Cd_xTe$ layer in the QDSL structures was estimated at ~2 nm, i.e., 6 ML (for CdTe, 1 ML = 0.324 nm). Taking into account the above-discussed similarity of the spectra of QDSL samples **b05** and **b50** and $ZnTe/Zn_{0.8}Cd_{0.2}Te$ sample **SL**, we take the composition parameter of the $Zn_{1-x}Cd_xTe$ alloy layer in QDSL samples **b05** and **b50** to be $x = 0.2$. The same is true for QDSL samples **b10.20** and **b10.200**. The thickness of the layer and the islands enriched with CdTe therein is 6 ML.

Let us consider one of the QDSL structures, **b50**. To perform the calculation, we must specify the composi-

tion of the alloy. Let the composition of the alloy in the island be $Cd_{0.7}Zn_{0.3}Te$. For the unstrained $Cd_{0.7}Zn_{0.3}Te$ alloy, we have $a = 6.369$ Å and $\omega_t = 143$ cm$^{-1}$. Then, for the $Cd_{0.7}Zn_{0.3}Te$/ZnTe pair, the lattice constant of the conjugated layers in the lateral direction is $a^{\perp} = 6.128$ Å, and the strain is $\Delta a/a = (6.128–6.369)/6.369$, in accordance with expression (4). For the CdTe-like vibration mode, we have $\Delta\omega_t/\omega_t = 3.03$, $\Delta a/a$ or $\Delta\omega_t/143 = 0.115$, and $\Delta\omega_t = +16$ cm$^{-1}$. The calculated frequency (143 + 16) cm$^{-1}$ and the observed frequency 156 cm$^{-1}$ of the CdTe-like vibration in QDSL structure **b50** are close to each other. Consequently, we can assume that the material of the QDs in sample **b50** is on average the $Cd_{0.7}Zn_{0.3}Te$ alloy. A similar calculation for the $Zn_{0.8}Cd_{0.2}Te$/ZnTe pair in sample **b50** yields the CdTe-like vibration frequency 151.5 cm$^{-1}$, comparable to the observed frequency 149 cm$^{-1}$. For the unstrained $Zn_{0.8}Cd_{0.2}Te$ alloy, the frequency of the CdTe-like mode is ~147 cm$^{-1}$. As to the ZnTe-like vibration modes, the observed 179 cm$^{-1}$ mode is the mode of the thick ZnTe buffer layer, whereas the 175 cm$^{-1}$ mode corresponds to two unresolved closed modes of two adjacent ZnTe and $Zn_{0.8}Cd_{0.2}Te$ layers. As discussed above, the $Zn_{0.8}Cd_{0.2}Te$ alloy layer is formed as a result of the relaxation of elastic strains on deposition of CdTe onto the ZnTe barrier layer. QDSL samples **b05** and **b50** differ from each other by the barrier layer's thickness; their lattice vibrations differ only slightly.

In contrast to structures **b05** and **b50** on the substrate with the ZnTe buffer layer, QDSL structures **b10.20** and **b10.200** were formed on substrate **b0** with the combined ZnTe(+CdTe) buffer layer. In structure **b0**, there is the CdTe layer with the thickness ~1 μm under the ZnTe buffer layer. The lattice's vibration mode of this strained (compressed) CdTe layer corresponds to the observed 149 cm$^{-1}$ mode. When superlattices **b10.20** and **b10.200** are deposited, the extra CdTe-like vibration mode at the frequency 144 cm$^{-1}$ appears. The frequency 144 cm$^{-1}$ is too low to belong to the elastically strained superlattice. For example, in QDSL structure **b50** considered above, the frequency of the mode is $\omega_t = 156$ cm$^{-1}$. Most probably, strains in QDSL structures **b10.20** and **b10.200** relaxed to a large extent via the formation of misfit dislocations. These structures are too complicated to perform the calculation similar to what is done for structure **b50**. By the example of QDSL samples **b10.20** and **b10.200**, it is clear how crucially the strains in the QDSL structures depend on the type of material of the buffer layer and its quality.

## 4. CONCLUSIONS

The multiperiod ZnTe/CdTe superlattices with the CdTe QDs are studied by the IR reflectance spectroscopy of lattice vibrations. The structures were grown by MBE on the GaAs substrate with the ZnTe buffer layer. In contrast to the previous study [5], in which no CdTe-like vibration modes were observed in similar structures grown on the substrate with the CdTe buffer layer, it is found possible to observe the CdTe-like vibration modes in the elastically strained layers of the superlattices with the ZnTe buffer layer. From the dispersion analysis of the spectra, it is established that, during deposition of CdTe on the formation of the superlattice of thin CdTe layers sandwiched between barrier ZnTe layers, the $Zn_{1-x}Cd_xTe$ alloy layer is formed. The composition of this alloy layer corresponds basically to $x \approx 0.2$; however, in the layer, there exist the $Zn_{1-x}Cd_xTe$ islands with an increased CdTe content. From theoretical estimations, it is established that, for some samples (**b05** and **b50**), the material of the islands (QDs) is the $Cd_{0.7}Zn_{0.3}Te$ alloy. For the pair of the elastically conjugated ZnTe/$Cd_{0.7}Zn_{0.3}Te$ layers, the frequency of the CdTe-like vibration mode in the $Cd_{0.7}Zn_{0.3}Te$ alloy increases from 143 cm$^{-1}$ (in the unstrained alloy) to 156 cm$^{-1}$ (observed experimentally). In these samples, relaxation of strains between the initial ZnTe and CdTe layers is accompanied by the formation of the elastically strained (compressed) dislocation-free $Cd_{0.7}Zn_{0.3}Te$ islands. In other samples, the frequency of the CdTe-like vibration mode is 144 cm$^{-1}$, only slightly different even from the frequency in unstrained CdTe, suggesting that the plastic deformation processes with the formation of misfit dislocations go on in the layers of these samples.

## ACKNOWLEDGMENTS

I am grateful to G. Karczewski (Institute of Physics, Poland) for the QDSL samples put at our disposal and to E. Makhov for the Fourier spectrometry measurements.

This study was supported in part by Program of the Presidium of the Russian Academy of Sciences "Low-Dimensional Quantum Structures" and the Russian Foundation for Basic Research, project no. 07-02-00899-a.

## REFERENCES

1. J. Tersoff and R. M. Tromp, Phys. Rev. Lett. **70**, 2782 (1993).
2. J. Tersoff, Phys. Rev. Lett. **81**, 3183 (1998).
3. H. Mathie, A. Chatt, J. Allegre, and J. P. Faurie, Phys. Rev. B **41**, 6082 (1990).
4. E. E. Onishchenko, V. S. Bagaev, V. V. Zaitsev, and E. I. Makhov, Physica E **26**, 153 (2005).
5. L. K. Vodop'yanov, S. P. Kozyrev, and G. Karchevski, Fiz. Tverd. Tela **45**, 1713 (2003) [Phys. Solid State **45**, 1798 (2003)].
6. V. S. Bagaev, L. K. Vodop'yanov, V. S. Vinogradov, V. V. Zaitsev, S. P. Kozyrev, N. N. Mel'nik, E. E. Onishchenko, and G. Karchevski, Fiz. Tverd. Tela **46**, 171 (2004) [Phys. Solid State **46**, 173 (2004)].

7. S. Mackowski, G. Karczewski, T. Wojtowicz, J. Kossut, S. Kret, A. Szczepanska, P. Dluzewski, G. Prechtl, and W. Heiss, Appl. Phys. Lett. **78**, 3884 (2001).
8. E. E. Onishchenko, V. S. Bagaev, G. Karczewski, S. P. Kozyrev, I. V. Kucherenko, N. N. Mel'nik, V. S. Vinogradov, and L. K. Vodop'yanov, Phys. Status Solidi C **3**, 881 (2006).
9. L. K. Vodop'yanov, S. P. Kozyrev, and Yu. G. Sadof'ev, Fiz. Tverd. Tela **45**, 1892 (2003) [Phys. Solid State **45**, 1990 (2003)].
10. H. W. Verleur, JOSA **58**, 1356 (1968).
11. V. S. Vinogradov, L. K. Vodop'yanov, S. P. Kozyrev, and Yu. G. Sadof'ev, Fiz. Tverd. Tela **41**, 1948 (1999) [Phys. Solid State **41**, 1786 (1999)].
12. P. Plumelle and M. Vandevyver, Phys. Status Solidi B **73**, 271 (1976).
13. L. K. Vodop'yanov, E. A. Vinogradov, A. M. Blinov, and V. A. Rukavishnikov, Fiz. Tverd. Tela **14**, 268 (1972) [Sov. Phys. Solid State **14**, 219 (1972)].
14. T. Fromherz, F. Hauzenberger, W. Faschinger, M. Help, P. Juza, H. Sitter, and G. Bauer, Phys. Rev. B **47**, 1998 (1993).
15. N. Peranio, A. Rosenauer, D. Gerthsen, S. V. Sorokin, I. V. Sedova, and S. V. Ivanov, Phys. Rev. B **61**, 16015 (2000).

*Translated by É. Smorgonskaya*